

Multiple Reference Frame-Based Control of Three-Phase PWM Boost Rectifiers under Unbalanced and Distorted Input Conditions

Peng Xiao, *Student Member, IEEE*, Keith A. Corzine, *Senior Member, IEEE*, and Ganesh Kumar Venayagamoorthy, *Senior Member, IEEE*

Abstract—Many control algorithms and circuits for three-phase pulse width modulation active rectifiers have been proposed in the past decades. In most of the research, it is often assumed that the input voltages are balanced or contain only fundamental frequency components. In this paper, a selective harmonic compensation method is proposed based on an improved multiple reference frame algorithm, which decouples signals of different frequencies before reference frame transformation. This technique eliminates interactions between the fundamental-frequency positive-sequence components and harmonic and/or negative-sequence components in the input currents, so that fast and accurate regulation of harmonic and unbalanced currents can be achieved. A decoupled phase-locked loop algorithm is used for proper synchronization with the utility voltage, which also benefits from the multiple reference frame technique. The proposed control method leads to considerable reduction in low-order harmonic contents in the rectifier input current and achieves almost zero steady-state error through feedback loops. Extensive experimental tests based on a fixed-point digital signal processor controlled 2 kW prototype are used to verify the effectiveness of the proposed ideas.

Index Terms—Active rectifier, harmonic compensation, multiple reference frame, phase-locked loop.

I. INTRODUCTION

THREE-PHASE voltage-source pulse width modulation (PWM) rectifiers have gained enormous popularity in the past two decades. In many motor drive and power supply applications, they have been replacing traditional diode/thyristor bridge rectifiers as the front end ac/dc interface due to their low line current distortion and high power factor. Although there are constant efforts to improve the power quality of diode/thyristor rectifiers, either through additional circuits [1]–[3] or using active filters [4], PWM rectifiers are still one of the most viable solutions for many applications, especially when bidirectional power flow is required [5].

The main benefits of PWM converters come from the fact that their switching devices operate at a frequency many times higher than the system fundamental frequency. This enables the converter to have fast response and close regulation of the dc voltage. Since the switching noise can be easily eliminated by passive filters, the supply currents drawn from the utility network are nearly

sinusoidal in normal conditions. In addition, the PWM rectifier can maintain good power factor through a wide load range.

The claim that PWM rectifiers draw little low-order harmonic current, however, is seldom true when the input voltages are unbalanced or contain harmonics. The three-phase power source, be it the power grid or a stand-alone generator, is rarely ideal in practical situations. If the rectifier control scheme is not designed properly to account for these non-ideal situations, the three-phase input currents can indeed contain low-order harmonics. It has been pointed out that with unbalanced input voltages the rectifier dc output voltage may contain second-order harmonic ripple, which in turn causes third-order non-zero-sequence harmonics in the input currents [6]. Although the magnitude of these harmonics is much lower compared to those generated by the diode/SCR counterparts, they can lead to lower power quality and may require additional passive filters to meet harmonic regulatory standards such as IEEE-519. Furthermore, non-ideal input voltage conditions may interfere with the converter controller and degrade its performance in achieving the two major objectives: dc voltage regulation and power factor correction. Laboratory experiments have shown that a large amount of harmonics in the line voltages can cause sub-harmonic resonance and affect the stability of the rectifier control.

The performance of PWM rectifiers under distorted input conditions varies greatly depending on the control scheme adopted. Harmonics and imbalance in the input voltages create a disturbance to the control, and very few control algorithms can provide a wide enough bandwidth to effectively suppress them. This is especially true for controls with slower current regulators.

Several methods have been proposed to improve the operation of PWM rectifiers under unbalanced input voltage conditions. Early research focused on the analysis of rectifier behavior under these conditions, and attempted to alleviate the situation by proper design of input inductors and dc capacitors [6]. In [7], a feed-forward control circuit was proposed, which used analog/digital components to generate appropriate PWM gating signals based on an unbalanced transfer matrix. Although the control had a simple implementation, its lack of feedback made the compensation sensitive to sensor errors and component variations. Based on symmetrical component theory, a feed-forward control strategy was proposed in [8] to eliminate harmonics caused by unbalanced input conditions. One of its main drawbacks is that unity power factor cannot be achieved. A dual current controller was proposed in [9], which utilized

Manuscript received October 3, 2007; revised January 30, 2008. Published July 7, 2008 (projected). Recommended for publication by Associate Editor S. Pekarek.

P. Xiao is with Thermadyne, Lebanon NH 03766 USA.

K. A. Corzine and G. K. Venayagamoorthy are with the Missouri University of Science and Technology, Rolla, MO 65409 USA (e-mail: keith@corzine.net).

Digital Object Identifier 10.1109/TPEL.2008.925205

two synchronous reference frames (SRFs) to separately regulate the positive and negative sequence currents. The use of two SRFs achieved very good control performance of the negative sequence components. However, the separation of the positive and negative SRFs was implemented with either low-pass filters or notch filters, whose limitations are detailed in Section III.

Some recently developed rectifier control algorithms also consider harmonics in the source voltages. A generalized model was derived in [10] to address the control issues caused by unbalanced and/or harmonic input conditions. Effects of harmonics on rectifier control were investigated in detail, but the compensation scheme only considered unbalanced inputs. Elimination of low-frequency harmonics in active rectifiers was also considered in [11], which attributed the sources of harmonics to pulse-width limits, improper PWM patterns and dead time. A predictive cancellation algorithm was proposed in [12] to reduce harmonics in the rectifier input currents. However, due to the algorithm's open-loop nature, its performance was sensitive to sensor errors and control time delay.

With advances in the design of active filter controls, a new trend in harmonic current regulation is the use of selective harmonic compensation techniques, which target only a selected group of harmonic components, instead of trying to regulate signals over a wide spectrum. These techniques can be roughly classified into two categories based on the frame of reference they employ, although it has been proven that some of the methods are just equivalent implementations in different reference frames [13], [14].

Several stationary reference frame based control methods have been proposed and found applications in active filters, voltage source rectifiers, uninterruptible power supplies (UPS), and static var compensators (STATCOMs) [13]–[19]. The majority of these techniques are based on a form of resonant notch filter transfer function. In some cases, an integrator or proportional-integrator (PI) stage is also incorporated in the transfer function. Another stationary frame based method was the adaptive selective harmonic elimination (ASHE) algorithm [20], which could eliminate certain harmonic components by slowly adjusting weight parameters using a least mean square algorithm.

The other category of selective harmonic control methods are based on rotating reference frames. In [21], Schauder *et al.* proposed a multiple reference frame based controller for active filters and power line conditioners. A similar implementation was set forth in [22] for active filter control.

In this paper, a novel control algorithm is proposed to eliminate the low-order harmonic components in the ac currents of grid-tied converters when input ac voltages are unbalanced or contain low-order harmonics. Based on multiple reference frame theory, the proposed method improves existing implementation to achieve faster dynamics and lower computational requirement. The main goal of the control is to produce high-quality balanced sinusoidal three-phase currents on the ac side in the presence of distorted input voltage conditions, thus avoid drawing harmonic or unbalanced currents from the utility system. The proposed harmonic elimination control method can be applied to both PWM rectifiers and grid-tied PWM inverters. In this paper, a 2 kW three-wire PWM boost rectifier system is used as an example to demonstrate its effectiveness.

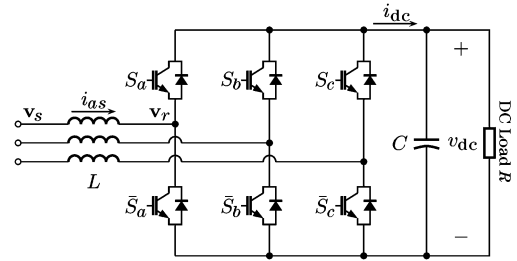


Fig. 1. Circuit diagram of a three-phase boost-type rectifier system.

The effects of distorted input conditions on rectifier control are briefly studied in Section II, in which the control objectives of the proposed technique are also defined. In Section III, the decoupled multiple reference frame algorithm is derived, and comparisons are made between existing techniques and the proposed method. Based on the MRF technique, a line synchronous algorithm is set forth in Section IV, where simulation results are used to demonstrate its effectiveness. Although the MRF-based harmonic compensation technique can be integrated with many basic rectifier control algorithms, a $P - Q$ decoupled control scheme is adopted in this work and illustrated in Section V. Implementation of the proposed algorithms in a digital signal processor (DSP) system is described in Section VI, where extensive test results are presented.

II. BEHAVIOR OF RECTIFIER CONTROL UNDER UNBALANCED AND DISTORTED CONDITIONS

A. Circuit Description

The typical circuit diagram of a three-phase PWM voltage source boost-type rectifier is shown in Fig. 1. Therein, the three legs of a three-phase IGBT bridge are connected to the power grid through an inductor L (with series resistance r). In most control schemes, the output dc voltage v_{dc} and the input source voltages $\mathbf{v}_s = [v_{as}, v_{bs}, v_{cs}]^T$ and currents $\mathbf{i}_s = [i_{as}, i_{bs}, i_{cs}]^T$ are sensed and then used to determine the proper PWM gating signals S_a, S_b, S_c and their complements. In a three-wire system as shown in Fig. 1, since there is no zero-sequence current path, the three-phase quantities are not independent. Therefore, only two line-to-line voltages (v_{ab} and v_{bc}) and two currents (i_{as} and i_{bs}) need to be sensed. Switching at a high frequency, the IGBT legs produce voltages at the rectifier terminals, whose average values $\mathbf{v}_r = [v_{ar}, v_{br}, v_{cr}]^T$ would form a set of three-phase balanced sinusoidal voltages under ideal conditions.

It should be noted that since there is no neutral wire, the zero-sequence ac current is always zero, no matter what source voltages are applied. Therefore, it is convenient in the following derivation to omit the zero-sequence component, and only q - and d -axis quantities are considered in each reference frame.

B. Synchronous Reference Frame Equivalent Circuit

A brief analysis of the behavior of the rectifier is helpful for the understanding of the effects of unbalanced and distorted input conditions. The state-space model of the above circuit can be established in the synchronous reference frame, in which the abc variables are transformed into qd variables in a rotating coordinate.

A two step transformation process is often seen in the literature, in which abc variables were first translated into stationary qd variables with a constant matrix, then translated into the synchronous reference frame with a time-varying matrix. In this paper, a direct approach is taken as follows:

$$\begin{bmatrix} f_q \\ f_d \end{bmatrix} = \frac{2}{3} \begin{bmatrix} \cos(\theta) & \cos(\theta - 2\pi/3) & \cos(\theta + 2\pi/3) \\ \sin(\theta) & \sin(\theta - 2\pi/3) & \sin(\theta + 2\pi/3) \end{bmatrix} \begin{bmatrix} f_a \\ f_b \\ f_c \end{bmatrix} \quad (1)$$

where f denotes any three-phase quantities such as voltages, currents, or flux linkages, and θ is the phase angle of the a -phase utility voltage \mathbf{v}_s . As mentioned earlier, it is assumed that zero-sequence component is negligible, therefore

$$f_c = -f_a - f_b. \quad (2)$$

The inverse transformation is

$$\begin{bmatrix} f_a \\ f_b \\ f_c \end{bmatrix} = \begin{bmatrix} \cos(\theta) & \sin(\theta) \\ \cos(\theta - 2\pi/3) & \sin(\theta - 2\pi/3) \\ \cos(\theta + 2\pi/3) & \sin(\theta + 2\pi/3) \end{bmatrix} \begin{bmatrix} f_q \\ f_d \end{bmatrix}. \quad (3)$$

The state-space equations for the ac side circuit are

$$\begin{aligned} Lp i_{qs} &= v_{qs} - i_{qs}r - \omega_e L i_{ds} - v_{qr} \\ Lp i_{ds} &= v_{ds} - i_{ds}r + \omega_e L i_{qs} - v_{dr} \end{aligned} \quad (4)$$

where p denotes differentiation with respect to time, $\omega_e = p\theta$ is the electrical angular speed of the utility voltage, and $[v_{qs}, v_{ds}]$, $[i_{qs}, i_{ds}]$ and $[v_{qr}, v_{dr}]$ are the results obtained when \mathbf{v}_s , \mathbf{i}_s , and \mathbf{v}_r are transformed into the synchronous reference frame, respectively.

For the dc side circuit, the following equation holds

$$Cpv_{dc} = i_{dc} - \frac{v_{dc}}{R}. \quad (5)$$

In (5), C is the capacitance of the dc linkage capacitor, and R is the equivalent resistance of the dc load. The two sides are related through instantaneous power balance

$$i_{dc} = \frac{3(v_{qr}i_{qs} + v_{dr}i_{ds})}{v_{dc}}. \quad (6)$$

Fig. 2 shows the ac side circuit diagram in the SRF. It can be shown that if the input voltages \mathbf{v}_s are balanced and free of harmonics, v_{qs} and v_{ds} become dc quantities. A controller can be designed to determine v_{qr} and v_{dr} , which are also dc quantities in steady state.

However, if the input voltages \mathbf{v}_s are unbalanced or contain harmonic components, v_{qs} and v_{ds} are no longer constant and contain a series of sinusoidal components, which act as disturbances to the system. In this case, the operating point of the system is no longer fixed, and the controller must have a very large bandwidth to suppress these disturbances, otherwise harmonic components will appear in the state variables, i.e., the input ac currents and output dc voltage. It should be noted that the input inductor of the rectifier circuit often has a relatively low inductance. Therefore, even a small amount of harmonics in \mathbf{v}_s can create large harmonic currents if \mathbf{v}_r does not have the same canceling components. To address the issue of non-ideal

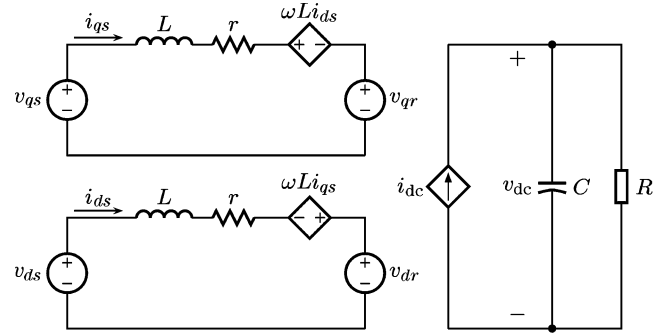


Fig. 2. Equivalent circuit diagram of the rectifier system in the synchronous reference frame.

input conditions, several approaches have been proposed [23]. The constant power method tries to maintain a constant input power (assuming the dc load is also constant), thus eliminating ripple in the output dc voltage. The constant resistance method regulates the rectifier so that it appears as a three-phase balanced resistive load. In this work, the control objective is to maintain balanced sinusoidal three-phase input currents, even when the input voltages are unbalanced and/or contain harmonics.

III. MULTIPLE REFERENCE FRAME HARMONIC CONTROL SCHEME

A. Overview of the Multiple Reference Frame Theory

The concept of multiple reference frames was set forth several decades ago and was initially used in the analysis of electric machinery. In [24], Krause established the basic architecture of MRF and considered its application in the analysis of symmetrical induction machines. It was shown that the MRF method allowed simplified steady-state analysis of machine operations under unbalanced or non-sinusoidal voltage conditions. Later, Sudhoff *et al.* presented MRF-based analysis of a variety of other electric machines, including unsymmetrical induction machines [25], multistack variable-reluctance stepper motors [26], and brushless dc motors [27]. These machines are difficult to model with conventional methods due to asymmetry or non-sinusoidal back emf. MRF provided a means to keep state variables of the model constant in steady state so that the model equations could be readily linearized. Recently, MRF was also employed in the identification of inter-turn faults in induction machine stators [28].

It is interesting to note that although MRF has found many applications as an analysis tool, its use in real-time controllers has not received much attention. This is primarily due to the fact that, 1) significant computation arises from the need for reference frame transformations; 2) the dynamic performance of most existing MRF based controllers is not satisfactory; and 3) accurate synchronization with utility voltage is required.

With the advances in modern DSP design, commercial off-the-shelf DSP chips today have greatly improved their computational power through increased clock speed and parallel operation. Thus the computational requirement is no longer a determining factor. Herein, the issues of performance and synchronization will be addressed.

B. Multiple Reference Frames for Arbitrary Three-Phase Signals

The synchronous reference frame is commonly used in the control of PWM rectifiers and inverters. By transforming the time-varying three-phase sinusoidal voltage and current signals to this rotating reference frame using (1), these signals become dc quantities in steady state. It is thus much easier to design the controller to achieve zero steady-state error. The same concept can be naturally extended to cases where the signals are unbalanced and/or contain harmonics. Let $\mathbf{v} = [v_a, v_b, v_c]^T$ be a set of three-phase periodic voltage signals with arbitrary waveforms. As long as all three signals are periodic with the same base frequency ω_e , each can be expressed as the sum of a series of harmonics using the Fourier transformation

$$v_j = \sum_{k=0}^{\infty} A_{jk} \cos(k\omega_e t + \phi_{jk}) \quad (7)$$

where $j = a, b$, and c ; A_{jk} and ϕ_{jk} are respectively the magnitude and phase angle of the k -th harmonic component in phase j . For each harmonic frequency $f_k = k\omega_e/2\pi$, symmetrical component theory can be applied. No matter what magnitude or phase angles each phase component has at this frequency, there exists three sets of symmetrical components that can uniquely represent the three-phase signals at f_k

$$\begin{aligned} & \begin{bmatrix} A_{ak} \cos(k\omega_e t + \phi_{ak}) \\ A_{bk} \cos(k\omega_e t + \phi_{bk}) \\ A_{ck} \cos(k\omega_e t + \phi_{ck}) \end{bmatrix} \\ &= A_k^+ \begin{bmatrix} \cos(k\omega_e t + \phi_k^+) \\ \cos(k\omega_e t + \phi_k^+ - 2\pi/3) \\ \cos(k\omega_e t + \phi_k^+ + 2\pi/3) \end{bmatrix} \\ &+ A_k^- \begin{bmatrix} \cos(k\omega_e t + \phi_k^-) \\ \cos(k\omega_e t + \phi_k^- + 2\pi/3) \\ \cos(k\omega_e t + \phi_k^- - 2\pi/3) \end{bmatrix} \\ &+ A_k^0 \begin{bmatrix} \cos(k\omega_e t + \phi_k^0) \\ \cos(k\omega_e t + \phi_k^0) \\ \cos(k\omega_e t + \phi_k^0) \end{bmatrix}. \quad (8) \end{aligned}$$

If the zero-sequence component is assumed to be zero, the harmonic contents at frequency f_k can be represented by two balanced sets of quantities with the same electrical angular velocity $k\omega_e$: one set ($A_k^+ \angle \phi_k^+$) has positive sequence and its vector rotates counterclockwise in the vector plane, while the other set ($A_k^- \angle \phi_k^-$) has negative sequence and its vector rotates in the clockwise direction.

From the above analysis, it is clear that a set of periodic three-phase quantities can be viewed as a sum of multiple rotating vectors in the vector plane. Generally speaking, for each harmonic frequency f_k ($k = 1, 2, \dots, \infty$), two vectors may exist that rotate at the same electrical angular velocity $k\omega_e$ but in opposite directions.

A reference frame can be intuitively viewed as a rotating coordinate in the vector plane, which has a q -axis and a perpendicular d -axis. The q - and d -axis quantities of a vector viewed in that reference frame are simply the projection of the vector onto the two axes. Reference frame transformation, in this sense, is a change of the viewer's perspective from the stationary coordinate to a rotating one.

As proven in [24], if a balanced set appears in any reference frame, there is another reference frame wherein this balanced set will appear as constants. Therefore, when \mathbf{v} is transformed into a reference frame that is rotating counterclockwise at velocity $k\omega_e$, the positive-sequence vector of the k -th harmonic in \mathbf{v} will appear as standing still because it is moving in the same velocity and direction as the reference frame. In other words, transformation of this vector gives constant q - and d -axis quantities. A positive sequence vector that is rotating at velocity $m\omega_e$ ($m \geq 0, m \neq k$) will appear as sinusoidal terms with a frequency of $2\pi(m - k)\omega_e$. A negative sequence vector that is rotating with $m\omega_e$ will appear as sinusoidal terms with a frequency of $2\pi(m + k)\omega_e$.

In summary, when the zero-sequence component is not considered, a periodic three-phase signal can be decomposed into a sum of balanced three-phase sets; each can be of different harmonic frequencies, and can have either positive sequence or negative sequence. For each harmonic set, there exists one and only one reference frame into which the component can be transformed to be dc. Conversely, when the signal is transformed into a specific reference frame, only one harmonic set becomes dc quantities, and all other sets become sinusoidal terms whose frequency is determined by the relative angular velocity between the set and the reference frame.

C. Existing MRF-Based Control Methods

One technique based on multiple reference frames for active filter control was proposed in [22], where a current regulator was constructed and each harmonic component was regulated on its own rotating reference frame. A similar technique was proposed in [21] which integrated a PI controller in the MRF structure for each frequency of interest. Although these methods are simple and straightforward to implement, they suffer from a serious drawback, i.e., interference between different reference frames.

As described earlier, a balanced harmonic set $A_m \angle \phi_m$ that is not in synchronization with the reference frame becomes sinusoidal terms after the transformation. The frequency of the terms is determined by the relative velocity of the set and reference frame, and their magnitude is unchanged by the transformation. In [21], the original three-phase signals were sent to each reference frame so that the transformation result contained not only the desired dc component, but also a variety of sinusoidal terms. This inevitably affects the accuracy and dynamic performance of the controller since even in steady state the state variables of the system were not constant. In each reference frame, the system was constantly perturbed by a group of sinusoidal disturbances.

One way to alleviate this situation is to attenuate at least the dominant component with filters, as was done in [22]. Therein, a low-pass filter was constructed to reduce the magnitude of the positive sequence fundamental components, which was the dominant one in the nonlinear load currents. The output signal of the filter was then processed by MRF. Although filters can indeed partially reduce interactions among reference frames, their use comes with a price, i.e. the degraded dynamic response of the system. This is especially true when simple low-order filters are used. In fact, as will be shown in the next section, a difficult compromise has to be made between the attenuation and dynamic performance.

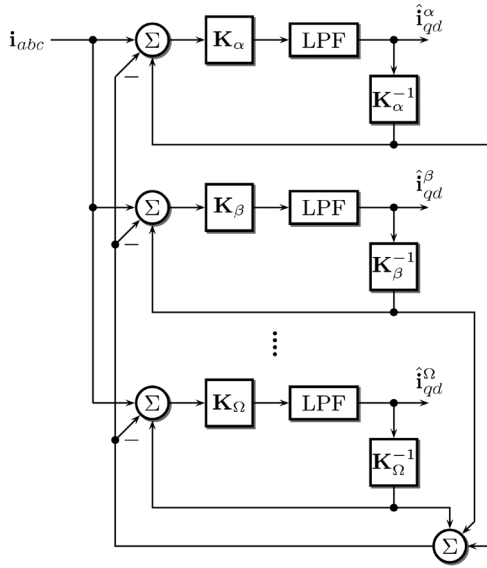


Fig. 3. Block diagram of the multiple reference frame estimator/regulator.

D. MRFSE

A novel multiple reference frame synchronous estimator/regulator (MRFSE) was set forth by Chapman and Sudhoff in [29]. The technique was applied to the optimal control of permanent magnet synchronous machine drives. Fig. 3 depicts the block diagram of the MRF synchronous estimator, which is essentially the same diagram as shown in Fig. 3 of [29], except that in the original figure an integrator with unity negative feedback was used, instead of a low-pass filter. It can be shown that the integrator with a unity negative feedback loop has a transfer function

$$H(s) = \frac{1}{s/G_e + 1} \quad (9)$$

which is identical to that of a first-order low-pass filter with unity dc gain and a cutoff frequency of G_e . Thus Fig. 3 can be seen as a generalized version of the MRF synchronous estimator in [29].

As can be seen in Fig. 3, a three-phase current signal is processed by several parallel channels, each representing a frame of reference ($\alpha, \beta, \dots, \Omega$). Unlike conventional MRF techniques which multiply the raw signal directly with transformation matrices ($\mathbf{K}_\alpha, \mathbf{K}_\beta, \dots, \mathbf{K}_\Omega$), MRFSE subtracts the sum of all estimated components from the original signal, and adds to it the estimated component resulted from the specific reference frame the signal is being transformed into. In the steady state, this feedback network allows only one component to pass through each reference frame, and that component is exactly the one that is in synchronization with the reference frame. Therefore, the scheme essentially decouples all the different reference frames so that the output of each channel contains only constant quantities, which are the q - and d -axis values of a balanced harmonic set that rotates synchronously with the reference frame. In other words, the MRFSE is capable of extracting cleanly each harmonic component in the input signal. This is a feature that can not be achieved by using either low-pass filters or notch filters. It is important to note that although harmonic contents considered in [29] were assumed to be balanced, the general idea can be extended to three-phase periodic signals with arbitrary waveforms. Formal mathematical justification was presented in [29], which

shows that the error of the estimator will converge exponentially to zero if the input is constant and all harmonic components are considered in the MRFSE structure. The rate of the convergence depends on the number of channels (n) and the low-pass filter. In the case of simple first-order low-pass filters, the decay rate is $n\omega_c$, where ω_c is the cutoff frequency of the filter.

Although MRFSE provided a fast and accurate means to estimate individual harmonic components in a three-phase periodic signal, it has not been widely adopted in practical applications. One drawback of the MRFSE implementation is that it requires very intensive computational power to perform the transformations of different reference frames. For each harmonic component, signals not only need to be transformed into the qd reference frame, they also need to be re-constructed by inverse transformation back into the abc forms. This would significantly increase the required computational efforts. Therefore, for practical implementation with DSPs, the MRFSE presents hardware and software challenges, especially when the number of harmonic channels is high.

E. Improved MRF Scheme

To apply MRFSE in rectifier control, one major challenge is to reduce the amount of calculations it requires. For three-phase utility-connected power converters, the following observations are made.

- 1) The most dominant component in the converter currents is the positive sequence fundamental frequency component, which can have a magnitude tens of times higher than that of harmonic components.
- 2) Imbalance can be a common phenomenon in the utility systems, and a high magnitude of negative sequence fundamental component may exist.
- 3) In most systems, even and triplen harmonics are not an issue. The dominant low-order harmonics are the fifth, seventh, 11th, 13th, etc. Furthermore, the higher the frequency is, the lower the magnitude is.
- 4) If the signals are balanced, the fifth, 11th, ... harmonics have a negative sequence, while the seventh, 13th, ... harmonics have a positive sequence [30].
- 5) If the signals are unbalanced, positive sequence fifth, 11th, etc. harmonics and negative sequence seventh, 13th, etc. harmonics may exist, but they have very low amplitudes.

Based on these observations, a modified MRF scheme is proposed in this paper. The block diagram of the scheme is shown in Fig. 4, where the superscript $1p$ is used to denote fundamental frequency positive sequence component, $1n$ stands for fundamental frequency negative sequence component, $5n$ stands for fifth harmonic negative sequence component, and so on.

Before the input current signal is transformed into reference frame $1p$, the output of reference frame $1n$ is reconstructed and subtracted from the input signal. Similarly, the output of reference frame $1p$ is reconstructed and subtracted from the input signal that goes into reference frame $1n$. The estimated $1p$ components are

$$\hat{\mathbf{i}}_{qd}^{1p} = LPF \left[\mathbf{K}_{1p} \left(\mathbf{i}_{abc} - \mathbf{K}_{1n}^{-1} \hat{\mathbf{i}}_{qd}^{1n} \right) \right] \quad (10)$$

and the estimated $1n$ components are

$$\hat{\mathbf{i}}_{qd}^{1n} = LPF \left[\mathbf{K}_{1n} \left(\mathbf{i}_{abc} - \mathbf{K}_{1p}^{-1} \hat{\mathbf{i}}_{qd}^{1p} \right) \right]. \quad (11)$$

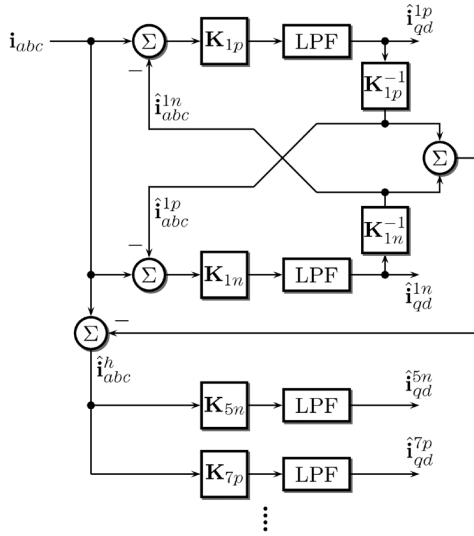


Fig. 4. Block diagram of the proposed multiple reference frame scheme.

Compared with MRFSER, it can be seen that only fundamental frequency components are involved in the feedback network, and no reconstruction of harmonic estimations is needed.

In this way, the input current is divided into three major components, 1) the positive sequence fundamental frequency component \hat{i}^{1p} , 2) the negative sequence fundamental component \hat{i}^{1n} caused by imbalance, and 3) the remaining components \hat{i}^h which are harmonics. All reference frames that process harmonics share the same input signal, which is

$$\hat{i}_{abc}^h = \mathbf{i}_{abc} - \hat{\mathbf{i}}_{abc}^{1p} - \hat{\mathbf{i}}_{abc}^{1n}. \quad (12)$$

If the input signal does not contain any harmonic components, this structure will cleanly extract the positive and negative sequence fundamental frequency components. Since harmonics are not considered in the feedback network, in reality there is some interference between different reference frames. However, the low magnitude of the harmonics means that their effects are small, as is shown below.

F. Simulation Results

To demonstrate the effectiveness of the proposed MRF scheme, a computer simulation was performed and comparisons were made between three MRF implementations, the conventional filter based method, MRFSER, and the proposed scheme.

In the simulation test, a 60 Hz three-phase voltage signal was processed with the three MRF schemes. In the signal, phase *a* had a magnitude of 197 V, which was 10% higher than that of phase *b* and *c*. In addition, the signal contained 5% negative sequence fifth harmonic component. To test the dynamic behavior of the methods, a step change occurred at time $t = 0.05$ s when the magnitude of the signal dropped by 30%.

The simulation results are shown in Fig. 5. Therein, the left column depicts the *q*-axis quantity of the extracted positive sequence fundamental components ($1p$), the right column depicts the extracted *q*-axis values of the negative sequence fundamental components ($1n$) and fifth-order harmonic component ($5n$).

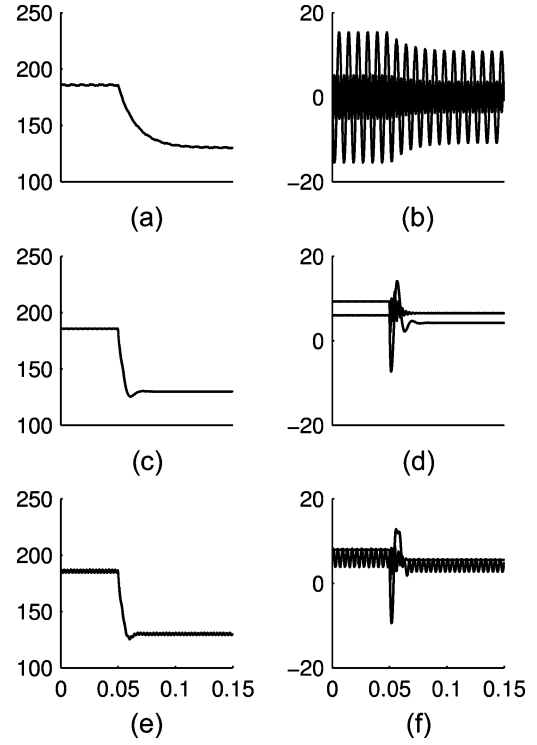


Fig. 5. Comparison of simulation results from three MRF-based methods. First row: conventional MRF; Second row: MRFSER; Last Row: proposed MRF scheme. Left column: estimated *q*-axis values of $1p$ component; Right column: estimated *q*-axis values of $1n$ and $5n$ components.

The two plots shown in the first row of Fig. 5 illustrate the results of the conventional MRF method. To reduce the interactions between different reference frames, a low-pass filter with cutoff frequency $\omega_c = 10$ Hz was used. It can be seen in Fig. 5(b) that the extracted $1n$ and $5n$ components still contain very large amount of ripple caused by the dominant $1p$ component. Although decreasing the cutoff frequency can reduce the amplitude of the ripple, it also further deteriorates the dynamic performance of the system, which is already very poor as shown in Fig. 5(a).

The results from the MRFSER method can be observed in the two plots shown in the second row of Fig. 5. In this study, a cutoff frequency of 60 Hz was selected for the low-pass filters. It is clear that MRFSER achieved much better dynamic performance and could completely eliminate interferences between different reference frames. In steady state, the estimated *q*-axis quantities are all constant values in each reference frame.

Finally, the traces in the bottom row of Fig. 5 depict the behavior of the proposed MRF algorithm, which used the same cutoff frequency as in the MRFSER study. The dynamic responses compare nearly identically to those of MRFSER. In steady state, there was only a small amount of high frequency ripple in the $1p$ and $1n$ component, which is expected due to the fact that $5n$ is not included in the feedback network. Because the $5n$ component has a much lower magnitude compared with fundamental frequency components, its effects on them were negligible in most cases. On the other hand, since the input signal to $5n$ reference frame has no $1p$ or $1n$ components, the transformation results are nearly dc quantities.

It is interesting to note that the $5n$ component becomes a 360 Hz sinusoid in the $1p$ reference frame, while it appears as a 240 Hz sinusoid in the $1n$ reference frame. Since the same cutoff frequency was used for all low-pass filters, the magnitude of the ripple in the $1n$ reference frame is higher than that in the $1p$ reference frame.

Based on the study, it can be concluded that although the proposed MRF may introduce some ripple caused by harmonics, their impacts are very limited in practical situations. The dominant components, which are often the ones with fundamental frequency, are decoupled and removed. The proposed method simplifies the MRFSEER structure and reduces computational requirement, without degrading dynamic performance.

It is important to mention that in some cases a harmonic component may have a high enough magnitude to cause large ripple in other reference frames, and the proposed MRF method can be readily modified to include that harmonic channel in the feedback network.

IV. MRF-BASED LINE SYNCHRONIZATION ALGORITHM

The tracking of phase and frequency information of the utility systems is an important aspect of most converter control algorithms that use the SRF technique. Although small variations of the estimated system frequency normally may not cause problems for the control of fundamental frequency signals, they can introduce a lot more ripple in the qd quantities of higher-order harmonics.

For example, an estimation error of 0.5 Hz for the fundamental component would cause an error of 6.5 Hz for the 13th harmonic reference frame, and it is very difficult to remove such ripple with simple low-pass filters while keeping good dynamic performance. Thus, to achieve good performance using MRF, the frequency of the utility system must be accurately tracked.

A commonly-used line-synchronization technique for three-phase applications is the synchronous reference frame phase locked loop (SRF-PLL) method [31], in which the source voltages are transformed into the qd rotating reference frame, and a feedback loop is used to regulate the angular position of the reference frame so that either the q - or d -axis component becomes zero. The SRF-PLL gives satisfactory performance under ideal input conditions, i.e. when the source voltage is balanced and free of harmonics. However, imbalance and distortions in the source voltage can cause large oscillations in the extracted frequency and phase information. Even though these oscillations can be attenuated by low-pass filters, this approach has a serious negative impact on the dynamic performance of the PLL. Therefore, this method is not appropriate for the proposed MRF-based harmonic compensation algorithm.

Recently, based on the conventional SRF-PLL, a novel improvement called the decoupled double synchronous reference frame PLL (DDSRF-PLL) was proposed [32], which utilized two synchronous reference frames to process the input voltages. The two reference frames have the same angular speed, but are rotating in opposite directions. Signals in the two reference frames are decoupled through a feedback network so that the interference between them can be totally eliminated. This key feature of the technique makes it possible to extract

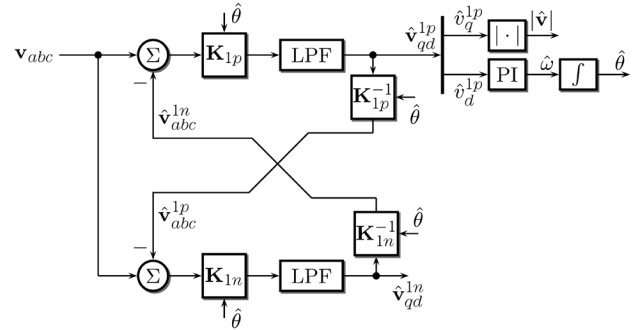


Fig. 6. Block diagram of the multiple reference frame based synchronization algorithm.

separately the fundamental-frequency positive-sequence component, which can then be used in the PLL stage. Through simulation and experimental results, the authors showed that the technique had excellent performance even when input voltages were highly unbalanced. The effect of harmonics on the PLL was also investigated and the results showed that they have very little impact.

In this paper, the same idea of DDSRF-PLL is adopted, but a different approach is taken for the implementation. Fig. 6 shows the control diagram of the proposed MRF-PLL scheme. It can be seen that the a decoupled MRF structure similar to the one shown in Fig. 4 is used. As discussed earlier, the decoupled MRF structure is able to extract precisely both the positive- and negative-sequence components of the fundamental-frequency voltage signals. The extracted positive sequence d -axis component is passed through a PI controller to generate an estimation of the angular speed of the component. The speed estimation, $\hat{\omega}$, is integrated to give the angular position $\hat{\theta}$, which is used in the transformation matrices for both positive and negative sequence reference frames.

Compared with DDSRF-PLL, the proposed MRF-based PLL method has a very straightforward implementation and almost identical performance. It can also be easily extended to include other harmonic components in the decoupling feedback structure if these components are large enough to degrade the PLL's performance.

A simulation was performed to verify the effectiveness of the proposed MRF-base PLL algorithm, in which the cutoff frequency of the low-pass filter was 60 Hz, and the parameters of the PI block were $K_p = 2.22$, and $K_i = 246.7$. Fig. 7 shows the responses of the MRF-PLL under various input voltage situations. Initially, the three-phase voltages were balanced and had a frequency of 48 Hz. At time $t = 0.5$ s, there was a step change in the utility frequency, which increased by 25% and became 60 Hz. The dynamics of the PLL under such a large step input can be clearly observed by looking at the estimated angular speed, which rapidly increased to the set value in less than one cycle. The effect of this step disturbance on the angular position $\hat{\theta}$ was even more attenuated due to the low-pass filtering effect of the integrator.

At time $t = 0.15$ s, the magnitude of phase a voltage was increased by 40%. This imbalance in magnitudes created negative sequence components in the source voltage. As can be seen in Fig. 7, the estimated electrical angular velocity only had a

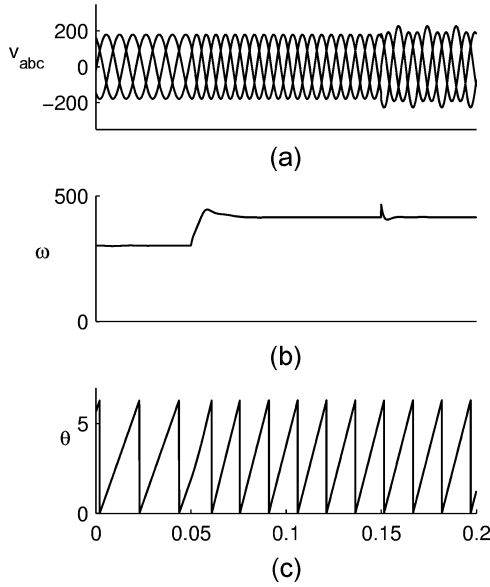


Fig. 7. Simulation results of the proposed MRF-based PLL algorithm. (a) Three-phase voltages (V). (b) Estimated electrical angular speed (rad/s). (c) Estimated phase angle (rad).

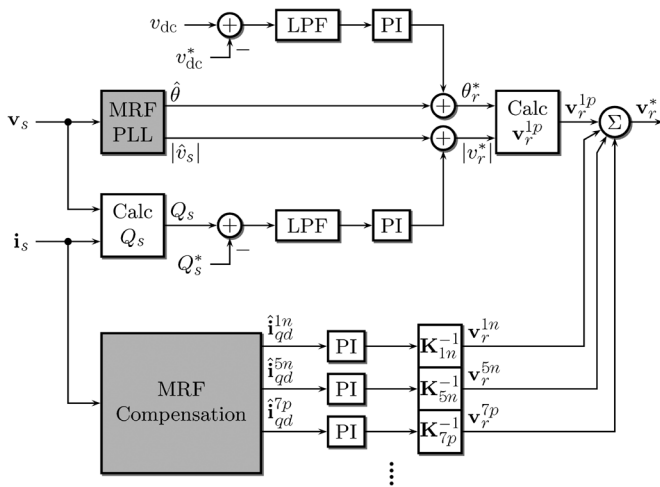


Fig. 8. Block diagram of the complete MRF-based active rectifier control.

short period of transient process, then quickly settled down to its nominal value of 377 rad/s. No visible distortion in the angular position $\hat{\theta}$ is observed.

V. THE COMPLETE CONTROL ALGORITHM

The complete block diagram of the proposed rectifier control algorithm is shown in Fig. 8. The details of the two grayed blocks, MRF Compensation and MRF-PLL, have already been described in previous sections. It can be observed that two parallel paths are used for the regulation of dc voltages and power factor. The reactive power is calculated directly from the three-phase voltages and currents with

$$Q = \frac{\sqrt{3}}{2} [v_{as}(i_{cs} - i_{bs}) + i_{as}(v_{bs} - v_{cs})]. \quad (13)$$

The estimated qd quantities in each reference frame are passed through a PI block, then transformed back into the abc frame and added to the rectifier voltage references. This guarantees that in steady state all the harmonic components become

zero. In this study, the negative sequence fundamental frequency component is also regulated to zero, which effectively maintains a balanced set of three-phase input currents even when the source voltage is unbalanced. It should be pointed out, however, that other control strategies for unbalanced input can also be used by setting appropriate reference currents for the $1p$ and $1n$ current components [9].

VI. EXPERIMENTAL RESULTS

A. Prototype Description

To experimentally verify the effectiveness of the proposed MRF-based technique, a 2 kW three-phase PWM boost-type rectifier prototype system was built in the laboratory. The system consists of a 1.2 mH three-phase input inductor, a rectifier bridge with six IGBTs (rated 600 V and 75 A), a dc link capacitor of 3900 μF , and a resistive dc load of 40 ohms. Hall effect voltage and current sensors were used to measure the output dc voltage (v_{dc}), input line-to-line voltages (v_{ab} and v_{bc}) and input currents (i_{as} and i_{bs}).

The IGBTs were controlled by a fixed-point DSP (TMS320F2812 from Texas Instruments) with a clock frequency of 150 MHz. The switching and control frequency was set to 20 kHz. In each control cycle, the DSP samples the sensed signals and completes all the calculations needed to determine the switching states. In addition, two D/A channels were used so that internal variables can be displayed on an oscilloscope.

The proposed MRF-based rectifier control algorithm was implemented on the DSP. In addition to positive and negative synchronous reference frames $1p$ and $1n$, three harmonic reference frames ($2n$, $5n$, and $7p$) were also used to target the second, fifth, and seventh harmonics, respectively. A flag variable was used so that the harmonic/imbalance compensation function can be turned on or off while the system is running.

Although voltages from the electric power grid can become unbalanced and contain harmonics due to nonlinear loads, the amount of distortion cannot be controlled. Therefore, to test the performance of the prototype system under various distorted conditions, a 5.25 kW three-phase programmable power supply (Elgar SW5250) was used as the input power source of the rectifier. The device can generate three-phase voltages of arbitrary phases and magnitudes, and the waveforms can be programmed using GPIB commands. It is thus very convenient to generate voltages with a controlled amount of imbalance and harmonics.

All the test results shown below were based on the following operating point: the line-to-line rms voltage of the power source is 120 V, the commanded dc link voltage is 280 V, and the rated load power is 1.96 kW.

B. Harmonic Compensation Test

In the first test, only harmonic components (fifth and seventh) were intentionally added to the source voltages, and the three phases are balanced. Fig. 9(a) shows the distorted input line-to-line voltages v_{ab} and v_{bc} , which contain 10% of fifth harmonic and 5% of seventh harmonic contents. It was mentioned in previous sections that if harmonic compensation algorithm is not used, even a small amount of low-order harmonic voltages can create highly distorted currents, which can be clearly seen in Fig. 9(b). As expected, when the compensation function is

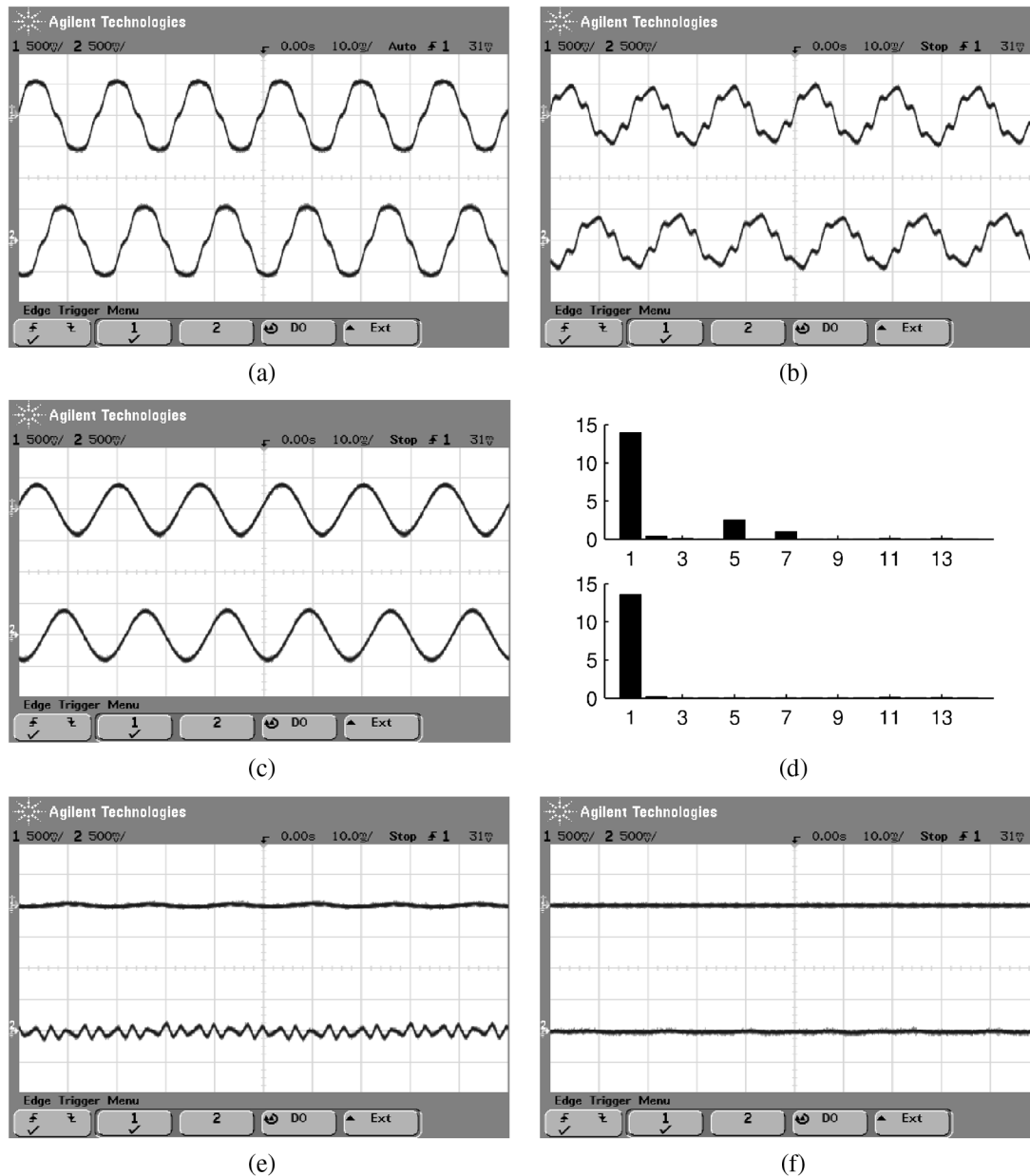


Fig. 9. Experimental results for test with balanced harmonic input voltages. (a) Line-to-line source voltages. (b) Input currents before compensation. (c) Input currents after compensation. (d) FFT results of phase a current before (top trace) and after (bottom trace) compensation. (e) In and harmonic components before compensation. (f) In and harmonic components after compensation.

turned on, the input currents (i_a and i_b) are much cleaner and become almost pure sinusoidal, as illustrated in Fig. 9(c).

The spectra of the phase a current before and after the compensation are shown in Fig. 9(d). As can be seen, the second, fifth, and seventh harmonic components are completely canceled by the MRF algorithm. With the compensation in effect, the THD of the input current is decreased from 19.5% to 1.7%.

In the proposed algorithm, the negative-sequence components and harmonic components in the source currents are separately extracted. Although these signals do not physically exist and can only be obtained through calculations, they are important indicators of the degree of distortions in the currents. Through a two-channel D/A converter, the waveforms of i_a^{1n} and i_a^h are shown on an oscilloscope. Fig. 9(e) and (f) show these signals before and after the compensation is used. In Fig. 9(e), only a very small negative sequence component (the top trace)

can be seen because the three-phase source voltages are mainly balanced. However, the harmonic component (the bottom trace), which includes the sum of all harmonics, indicates that the input currents are highly distorted. In Fig. 9(f), with the help of the MRF-based harmonic compensation method, both the negative-sequence and harmonic traces are very close to zero, indicating a relatively clean current waveform.

C. Unbalanced Harmonic Cases

Next, unbalanced conditions were added to the source voltages, which still contain the same amount of harmonics as in the previous test. In this case, the magnitude of the phase a voltage was decreased from 70 V to 50 V, which is a 28% reduction. The magnitudes of phase b and c voltages remained the same.

To better illustrate this magnitude difference, the waveforms of line-to-line voltages v_{ab} and v_{bc} are placed on the same level

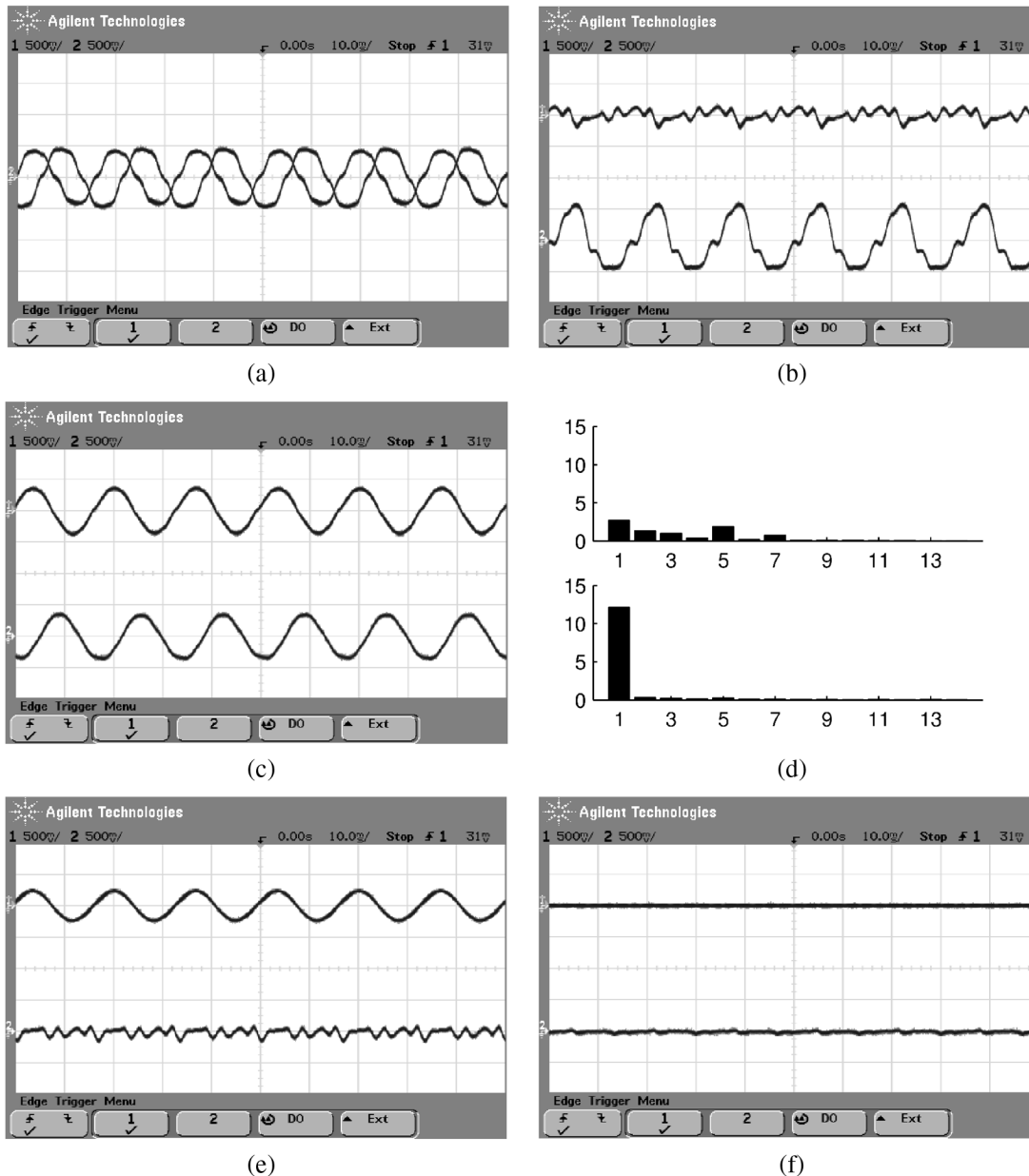


Fig. 10. Experimental results for test with unbalanced harmonic input voltages: (a) line-to-line source voltages; (b) Input currents before compensation; (c) Input currents after compensation; (d) FFT results of phase a current before (top chart) and after (bottom chart) compensation; (e) I_n and harmonic components before compensation; and (f) I_n and harmonic components after compensation.

in Fig. 10(a). The effects of this voltage imbalance and harmonics seriously degraded the performance of the rectifier control. As can be seen in Fig. 10(b), not only did the input currents have large amount of fifth and seventh harmonics, other harmonic components (second, third, fourth, etc.) also appeared. Due to the unbalanced input voltage, the magnitude of i_a (top trace) was much lower than that of i_b (bottom trace).

Fig. 10(c) shows the input current waveforms when the MRF-based compensation function is in effect. Apparently, the shapes of the waveforms are considerably improved. FFT calculations showed that the three targeted harmonic components were adequately compensated, and the magnitude of these harmonics were close to zero, as illustrated in Fig. 10(d). The harmonic and imbalance compensation control achieved a great decrease in THD of the phase a current, which reduced from 98.7% to

4.4%. Fig. 10(e) and (f) show the extracted negative-sequence and harmonic components in the input current. Without compensation, there exists a large amount of negative sequence current. Fig. 10(f) clearly shows that the compensation method can effectively balance the input currents.

It should be noted that because the harmonics are also unbalanced, they contain both positive and negative sequence components, and in theory two compensation channels should be used for each harmonic frequency to achieve complete compensation. However, in general the amount of non-typical harmonic components (positive fifth and negative seventh) are much smaller than those typical harmonic components (negative fifth and positive seventh). This fact justified the decision in the DSP program to only target the dominant typical harmonic components. On the other hand, if a specific harmonic component is particu-

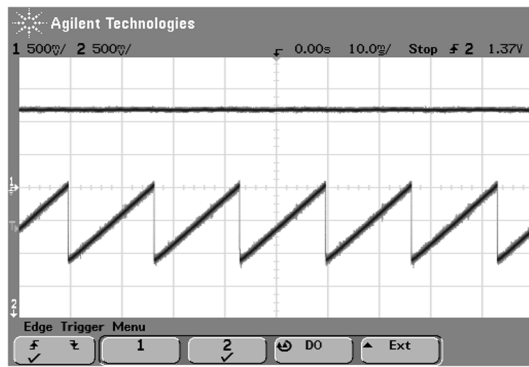


Fig. 11. Experimental results of the MRF-PLL algorithm under unbalanced and harmonic input conditions. Top trace: estimated q -axis values in $1p$ reference frame; Bottom trace: estimated phase angle.

larly large, or a resonant condition is observed, a dedicated compensation channel should be added to the MRF-based algorithm.

D. Performance of MRF-PLL

It is noteworthy to look at the performance of the MRF-based PLL algorithm under unbalanced and harmonic input voltage conditions. Fig. 11 depicts waveforms of the estimated q -axis voltage in $1p$ reference frame (whose absolute value is equal to the magnitude of the input voltage) and the estimated phase angle. These were both internal variables in the DSP algorithm and brought out using D/A channels. The voltages used for this experiment contain a large amount of fifth and seventh harmonics; they also contain a large amount of negative sequence components, which normally have a negative impact on the identification of voltage phase information.

Fig. 11 shows that the estimated phase angle and magnitude have very little ripple. This result is expected since the MRF-PLL decouples the interaction between positive and negative sequence components of the fundamental-frequency source voltage. Due to the low-pass filtering effect of the integrator, the harmonics have almost no visible impact on the phase angles. Some harmonic ripple may still appear in the magnitude waveform, even though they are attenuated by the LPF.

E. Dynamic Response Test

The fast dynamic response feature of the proposed MRF-based compensation algorithm can be appreciated by investigating its transient behavior. Fig. 12 depicts waveforms of the input currents (i_a and i_b) when there was a sudden turn-on of the algorithm. Before compensation, the unbalanced and distorted nature of the currents can be clearly seen. When the algorithm was turned on at time $t = 200$ ms, i_a and i_b became balanced and free of low-order harmonics almost instantly, only after a short period of transient process.

VII. CONCLUSION

A multiple reference frame based harmonic compensation algorithm for grid-connected three-phase power converter applications has been presented in this paper. A decoupled multiple reference frame architecture is proposed to eliminate interferences between components of different frequencies, which enables the selective compensation of dominant harmonic currents. Furthermore, a MRF-PLL technique was set forth to pre-

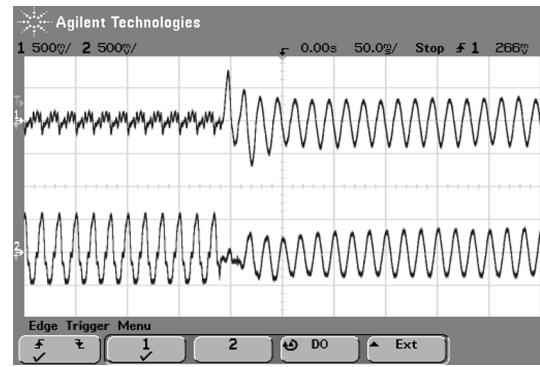


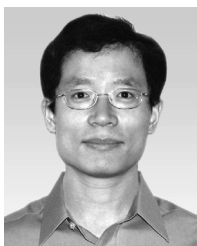
Fig. 12. Experimental results of the dynamic performance test. Compensation algorithm is turned on at time $t = 200$ ms. Top trace: phase a current; Bottom trace: phase b current.

cisely track the frequency and phase information of the utility system. The presence of imbalance or distortion in the source voltages does not degrade the performance of the phase-locked loop operation. The decoupled structure can cleanly extract the fundamental positive sequence component without sacrificing good dynamic performance. A complete experimental evaluation based on a three-phase rectifier system demonstrated that the proposed technique can yield fast and accurate operation. Balanced sinusoidal input currents can be achieved even under severe unbalanced and harmonic input conditions.

REFERENCES

- [1] P. Pejovi and Z. Janda, "An analysis of three-phase low-harmonic rectifiers applying the third-harmonic current injection," *IEEE Trans. Power Electron.*, vol. 14, no. 3, pp. 397–407, May 1999.
- [2] D. Alexa, A. Sirbu, and A. Lazar, "Three-phase rectifier with near sinusoidal input currents and capacitors connected on the ac side," *IEEE Trans. Ind. Electron.*, vol. 53, no. 5, pp. 1612–1620, Oct. 2006.
- [3] B. M. Saied and H. I. Zynal, "Minimizing current distortion of a three-phase bridge rectifier based on line injection technique," *IEEE Trans. Power Electron.*, vol. 21, no. 6, pp. 1754–1761, Nov. 2006.
- [4] H. Fujita and H. Akagi, "An approach to harmonic current-free AC/DC power conversion for large industrial loads: The integration of a series active filter with a double-series diode rectifier," *IEEE Trans. Ind. Applicat.*, vol. 33, no. 5, pp. 1233–1240, Sep./Oct. 1997.
- [5] S. Kwak and H. A. Toliyat, "Design and rating comparisons of PWM voltage source rectifiers and active power filters for AC drives with unity power factor," *IEEE Trans. Power Electron.*, vol. 20, no. 5, pp. 1133–1142, Sep. 2005.
- [6] L. Moran, P. D. Ziogas, and G. Joos, "Design aspects of synchronous PWM rectifier-inverter system under unbalanced input voltage conditions," *IEEE Trans. Ind. Applicat.*, vol. 28, no. 6, pp. 1286–1293, Nov./Dec. 1992.
- [7] D. Vincenti and H. Jin, "A three-phase regulated PWM rectifier with on-line feedforward input unbalance correction," *IEEE Trans. Ind. Electron.*, vol. 41, no. 5, pp. 526–532, Oct. 1994.
- [8] A. V. Stankovic and T. A. Lipo, "A novel control method for input output harmonic elimination of the PWM boost type rectifier under unbalanced operating conditions," *IEEE Trans. Power Electron.*, vol. 16, no. 5, pp. 603–611, Sep. 2001.
- [9] H. Song and K. Nam, "Dual current control scheme for PWM converter under unbalanced input voltage conditions," *IEEE Trans. Ind. Electron.*, vol. 46, no. 5, pp. 953–959, Oct. 1999.
- [10] P. Rioual, H. Pouliquen, and J. P. Louis, "Regulation of a PWM rectifier in the unbalanced network state using a generalized model," *IEEE Trans. Power Electron.*, vol. 11, no. 3, pp. 495–502, May 1996.
- [11] J. Wu, F. C. Lee, and D. Boroyevich, "Elimination of low-frequency harmonics caused by PWM in a three-phase soft-switched boost rectifier," *IEEE Trans. Ind. Applicat.*, vol. 38, no. 2, pp. 483–489, Mar./Apr. 2002.
- [12] P. Xiao, K. A. Corzine, and G. K. Venayagamoorthy, "Cancellation predictive control for three-phase PWM rectifiers under harmonic and unbalanced input conditions," in *Proc. Conf. IEEE Ind. Electron. Soc.*, 2006, pp. 1816–1821.

- [13] M. J. Newman, D. N. Zmood, and D. G. Holmes, "Stationary frame harmonic reference generation for active filter systems," *IEEE Trans. Ind. Appl.*, vol. 38, no. 6, pp. 1591–1599, Nov./Dec. 2002.
- [14] P. Mattavelli, "Synchronous-frame harmonic control for high-performance AC power supplies," *IEEE Trans. Ind. Appl.*, vol. 37, no. 3, pp. 864–872, May/Jun. 2001.
- [15] Y. Sato, T. Ishizuka, K. Nezu, and T. Kataoka, "A new control strategy for voltage-type PWM rectifiers to realize zero steady-state control error in input current," *IEEE Trans. Ind. Appl.*, vol. 34, no. 3, pp. 480–486, May/Jun. 1998.
- [16] D. N. Zmood and D. G. Holmes, "Stationary frame current regulation of PWM inverters with zero steady-state error," *IEEE Trans. Power Electron.*, vol. 18, no. 3, pp. 814–822, May 2003.
- [17] D. N. Zmood, D. G. Holmes, and G. H. Bode, "Frequency-domain analysis of three-phase linear current regulators," *IEEE Trans. Ind. Appl.*, vol. 37, no. 2, pp. 601–610, Mar./Apr. 2001.
- [18] X. Yuan, W. Merk, H. Stemmler, and J. Allmeling, "Stationary frame generalized integrators for current control of active power filters with zero steady-state error for current harmonics of concern under unbalanced and distorted conditions," *IEEE Trans. Ind. Appl.*, vol. 38, no. 2, pp. 523–532, Mar./Apr. 2001.
- [19] S. Fukuda and R. Imamura, "Application of a sinusoidal internal model to current control of three-phase utility-interface converters," *IEEE Trans. Ind. Electron.*, vol. 52, no. 2, pp. 420–426, Apr. 2005.
- [20] V. Blasko, "A novel method for selective harmonic elimination in power electronic equipment," *IEEE Trans. Power Electron.*, vol. 22, no. 1, pp. 223–228, Jan. 2007.
- [21] C. D. Schauder and S. A. Moran, "Multiple Reference Frame Controller for Active Filters and Power Line Conditioners," U.S. Patent 5 309 353, May 1994.
- [22] S. J. Lee and S. K. Sul, "A harmonic reference frame based current controller for active filter," in *Proc. IEEE Appl. Power Electron. Conf.*, 2000, pp. 1073–1078.
- [23] A. Jin, H. Li, and S. Li, "A flexible input currents control strategy for three-phase pfc rectifier under unbalanced system," in *Proc. IEEE Ind. Electron. Appl. Conf.*, 2006, pp. 1–6.
- [24] P. C. Krause, "Method of multiple reference frames applied to the analysis of symmetrical induction machinery," *IEEE Trans. Power Appar. Syst.*, vol. pas-87, no. 1, pp. 218–227, Jan. 1968.
- [25] S. D. Sudhoff, "Multiple reference frame analysis of an unsymmetrical induction machine," *IEEE Trans. Energy Conversion*, vol. 8, no. 3, pp. 425–432, Sep. 1993.
- [26] S. D. Sudhoff, "Multiple reference frame analysis of a multistack variable-reluctance stepper motor," *IEEE Trans. Energy Conversion*, vol. 8, no. 3, pp. 418–424, Sep. 1993.
- [27] P. L. Chapman, S. D. Sudhoff, and C. A. Whitecomb, "Multiple reference frame analysis of nonsinusoidal brushless DC drives," *IEEE Trans. Energy Conversion*, vol. 14, no. 3, pp. 440–446, Sep. 1999.
- [28] S. M. Cruz and A. J. Cardoso, "Multiple reference frames theory: A new method for the diagnosis of stator faults in three-phase induction motors," *IEEE Trans. Energy Conversion*, vol. 20, no. 3, pp. 611–619, Sep. 2005.
- [29] P. L. Chapman and S. D. Sudhoff, "A multiple reference frame synchronous estimator/regulator," *IEEE Trans. Energy Conversion*, vol. 15, no. 2, pp. 197–202, Jun. 2000.
- [30] *IEEE Recommended Practices and Requirements for Harmonic Control in Electrical Power Systems*, IEEE Std. 519-1992, Apr. 1993.
- [31] V. Kaura and V. Blasco, "Operation of a phase locked loop system under distorted utility conditions," *IEEE Trans. Ind. Appl.*, vol. 33, no. 1, pp. 58–63, Jan./Feb. 1997.
- [32] P. Rodriguez, J. Pou, and J. Bergas *et al.*, "Decoupled double synchronous reference frame pll for power converters control," *IEEE Trans. Power Electron.*, vol. 22, no. 2, pp. 584–592, Mar. 2007.



Peng Xiao (S'04) received the B.S.E.E. degree from Chongqing University, Chongqing, China in 1997, the M.S.E.E. degree from North China Electric Power University, Beijing, China, in 2000, the M.S.E.E. degree from the University of Wisconsin-Milwaukee, in 2004, and the Ph.D. degree in electrical engineering from the University of Missouri-Rolla in 2007.

He is currently a Senior Electrical Engineer at Thermal Dynamics Corporation, West Lebanon, NH. His research interests include power electronics, motor controls, soft-switching, and PFC techniques.



Keith A. Corzine (S'92–M'97–SM'06) received the B.S.E.E., M.S.E.E., and Ph.D. degrees from the University of Missouri-Rolla in 1992, 1994, and 1997, respectively.

He taught at the University of Wisconsin, Milwaukee, from 1997 to 2004 and is now an Associate Professor at the Missouri University of Science and Technology, Rolla, and co-Director of the Real-Time Power and Intelligent Systems Research Laboratory. He has published 31 refereed journal papers, nearly 50 refereed international conference papers, and

holds two U.S. patents related to multilevel power conversion. His research interests include power electronics, motor drives, naval ship propulsion systems, and electric machinery analysis.

Dr. Corzine received the Faculty Excellence award from the University of Missouri-Rolla in 2006 and the Excellence in Research Award from the University of Wisconsin-Milwaukee in 2001. He is currently the IEEE St. Louis Section Treasurer and the St. Louis Section IAS Chapter co-Chair.



Ganesh Kumar Venayagamoorthy (S'91–M'97–SM'02) received the B.Eng. degree (with honors) in electrical and electronics engineering from Abubakar Tafawa Balewa University, Bauchi, Nigeria, in 1994, and the M.Sc.Eng. and Ph.D. degrees in electrical engineering from the University of KwaZulu Natal, Durban, South Africa, in 1999 and 2002, respectively.

He was a Senior Lecturer with the Durban University of Technology, Durban, South Africa, prior to joining the Missouri University of Science and Technology (Missouri S&T), Rolla, in 2002. Currently, he

is an Associate Professor of Electrical and Computer Engineering and Director of the Real-Time Power and Intelligent Systems Laboratory, Missouri S&T. He was a Visiting Researcher with ABB Corporate Research, Vasteras, Sweden, in 2007. He has published two edited books, five book chapters, 55 refereed journal papers, and over 200 refereed international conference proceeding papers. His research interests are the development and applications of computational intelligence for real-world applications, including power systems stability and control, alternative sources of energy, FACTS devices, power electronics, sensor networks, collective robotic search, signal processing and evolvable hardware.

Dr. Venayagamoorthy was an Associate Editor of the IEEE TRANSACTIONS ON NEURAL NETWORKS (from 2004 to 2007) and the IEEE TRANSACTIONS ON INSTRUMENTATION AND MEASUREMENT (2007). He received the 2007 U.S. Office of Naval Research Young Investigator Program Award, the 2004 NSF CAREER Award, the 2006 IEEE Power Engineering Society Walter Fee Outstanding Young Engineer Award, the 2006 IEEE St. Louis Section Outstanding Section Member Award, the 2005 IEEE Industry Applications Society (IAS) Outstanding Young Member Award, the 2005 SAIEE Young Achievers Award, the 2004 IEEE St. Louis Section Outstanding Young Engineer Award, the 2003 INNS Young Investigator Award, the 2001 IEEE CIS Walter Karplus Summer Research Award, five prize papers from the IEEE IAS and IEEE CIS, a 2007 MST Teaching Commendation Award, a 2006 MST School of Engineering Teaching Excellence Award, and a 2007/2005 MST Faculty Excellence Award. He is listed in the 2007, 2008, and 2009 editions of *Who's Who in America*, 2008 edition of *Who's Who in the World*, and 2008 edition of *Who's Who in Science and Engineering*. He is a Senior Member of the South African Institute of Electrical Engineers (SAIEE). He is also a member of the International Neural Network Society (INNS); The Institution of Engineering and Technology, U.K.; and the American Society for Engineering Education. He is currently the IEEE St. Louis Computational Intelligence Society (CIS) and IAS Chapter Chairs, the Chair of the Working Group on Intelligent Control Systems, the Secretary of the Intelligent Systems subcommittee, and the Vice-Chair of the Student Meeting Activities subcommittee of the IEEE Power Engineering Society, and the Chair of the IEEE CIS Task Force on Power System Applications. He has organized and chaired several panels, invited and regular sessions, and tutorials at international conferences and workshops. He is General Chair of 2008 IEEE Swarm Intelligence Symposium and Program Chair of the 2009 IEEE-INNS International Joint Conference on Neural Networks.